AN EXPERIMENTAL APPROACH TO VORTEX-FLAME INTERACTION IN KARMAN VORTEX STREETS BEHIND A ROD-ARRAY

Norio Ohiwa
Graduate School of Engineering,
Nagoya Institute of Technology
Gokiso-cho, Showa-ku, Nagoya 466-8555, Japan
oiwa.norio@nitech.ac.jp

Yojiro Ishino
Graduate School of Engineering,
Nagoya Institute of Technology
Gokiso-cho, Showa-ku, Nagoya 466-8555, Japan
ishino@nitech.ac.jp

ABSTRACT

Structure and behavior of the spark-ignited propane-air premixed flames established in the quasi-turbulent and quiescent wake, which is generated by quickly moving a fine rod-array vertically downward in the quiescent stoichiometric propane-air mixture, are observed and analyzed using the tomography and PTV method. It is found that the quasi-turbulent and quiescent wake proposed here is composed of Karman vortex streets with the characteristic length scale ranging 0.2 ~ 0.5 mm and the tangential velocity of 4.0 m/s, and that it satisfies rather small and intense turbulence conditions of $l_d/\delta_L \approx 1$ and $v_\theta/S_L \approx 10$. Since the interface between the unburnt and burnt gases exhibits complicated and rugged appearances and consists of a continuous series of wrinkled laminar flame elements having the length scale ranging 0.2 ~ 2 mm, the turbulent flame initiated in the quasi-turbulent and quiescent wake with the moderately intense turbulence conditions of $l_d/\delta_L \approx 1$ and $v_\theta/S_L \approx 10$ is classified into the finely wrinkled laminar flame.

INTRODUCTION

Structure of turbulent premixed flames is well-known to be greatly affected by the turbulence properties of the mixture flow. Some typical models of the turbulent flame structure (Ballal and Lefevre, 1975, Bradley, 1992, Peters, 1999, Poinsot et al., 1991) are proposed using the non-dimensional characteristic parameters u'/S_L and l/δ_L, where u' and S_L indicate the turbulence intensity and the laminar burning velocity, and l and δ_L mean the turbulence length scale and the laminar flame thickness, respectively. Depending on whether $u'/S_L \ll 1$ and $l/\delta_L \gg 1$ or $u'/S_L \gg 1$ and $l/\delta_L \ll 1$, two extreme flame models are imaged; the wrinkled laminar flame model and the distributed reaction zone model, respectively. With respect to the flame structure in the intermediate condition between the two extremes, however, no consistent and reasonable model is proposed, although much attention is focused from the theoretical and practical points of view. This is because that the intermediate condition includes practically too wide range of turbulence properties to carry out detailed observation of the vortex-flame interaction under consistently subdivided ranges of turbulence conditions. In order to constitute a consistent set of turbulent flame models in the intermediate range of turbulence conditions between the two extremes, therefore, further experimental observations and analyses should be systematically made of the interdependency between the concrete processes of the vortex-flame interaction and the subdivided turbulence conditions, for example, by varying the characteristic length scale as $l/\delta_L > 1$, $l/\delta_L \approx 1$ and $l/\delta_L < 1$ under the moderately intense turbulence condition of $u'/S_L > 1$.

From the above-mentioned view point, the main objective of this paper is to examine experimentally the interactions between a laminar combustion wave with a cluster of vortices, not with a single vortex, under the subdivided turbulence conditions of $u'/S_L > 1$ and $l/\delta_L \approx 1$. To simplify observation and explanation of the flame structure and behavior, a wake behind a quickly downward moved rod-array in the quiescent mixture, which is apparently two-dimensional and is composed of a mutually arranged regular array of Karman vortex streets having nearly equal length scale with each other, is first selected as the turbulent flow field where flames will be established. This flow is named as "the quasi-turbulent and quiescent wake" in this paper, for lack of the randomness and three-dimensionality peculiar to turbulence.

A stoichiometric propane-air premixed flame is initiated in the quasi-turbulent and quiescent wake by a spark ignition and interacts with an array of vortex tubes, as it propagates radially in the wake. In this paper, concrete time histories of the vortex-flame interaction are optically observed and analyzed. Profiles of CH-emission intensity fluctuation of the propagating flames are also measured. In the optical observation an

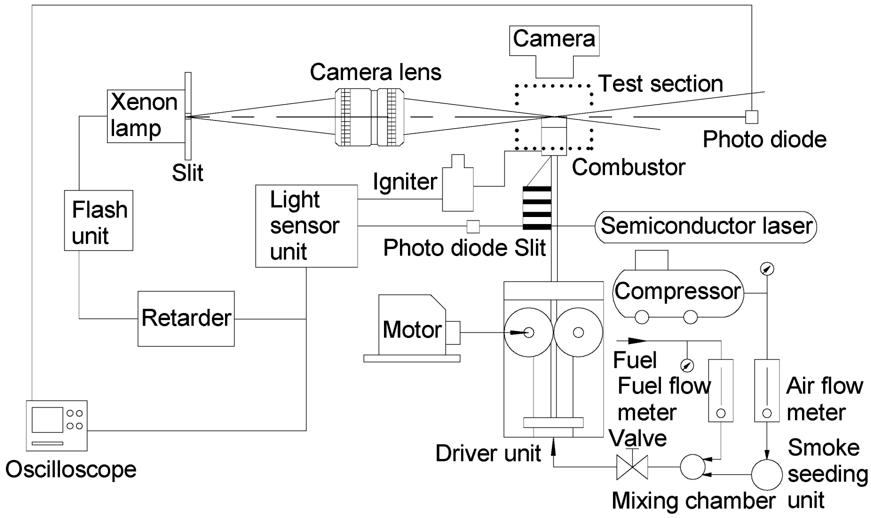

Fig. 1 Schematic diagram of the apparatus and the outline of the system construction

original device is introduced for making possible easy and clear explanations of the vortex-flame interaction.

EXPERIMENTAL APPARATUS AND METHODS

A schematic diagram of the experimental apparatus is presented in Fig. 1, and the structural details and dimensions of the rod-array and a set of spark needles are also shown in Fig. 2. The apparatus consists of a combustion test section including the rod-array, a rod-array driving unit, a mixture supply line, an optical system for CH-emission intensity measurement, and two types of optical systems.

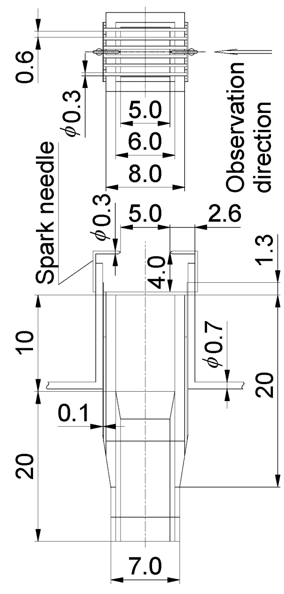

Fig. 2 Construction and dimensions of the rod-array, the spark needles and the observation direction

As shown in Fig. 2, the rod-array is constructed using six parallel cylindrical rods of 0.3 mm diameter, 8.0 mm length and 0.6 mm spacing, and is fixed to the exit section of a rectangular pipe. The latter has an inner and outer sectional area of 5.0 mm × 5.0 mm and 6.0 mm × 6.0 mm, respectively, and a length of 550 mm. A pair of spark needles, made of brass wire of 0.3 mm diameter and 2.6 mm length, has a gap of 5.0 mm and is installed at the central position 4.0 mm upward from the exit section with the axis parallel to the rods.

Air supplied by a blower and propane from a cylinder (commercial grade propane of 96.4 % purity) are metered individually and mixed to form stoichiometric mixture, and filled into the rectangular pipe. After being filled with the stoichiometric propane-air mixture, the rectangular pipe with the rod-array at its top end is rapidly moved vertically downward by the driving unit. Triggered by a signal generated from the laser light system, which is composed of a semiconductor laser, a light shield plate with three transparent stripes of 5.75 mm spacing, a photo-diode and a light sensor unit, the spark needles are discharged in the quasi-turbulent and quiescent wake, resulting in a turbulent combustion wave.

Three typical stages of one combustion experiment are illustrated in Fig. 3; (a) filling-up of mixture, (b) rapid downward movement of the rod-array and formation of the quasi-turbulent and quiescent wake, and (c) flame propagation after the spark ignition. U_g written in the figure indicates the average rod-array velocity of downward movement and is calculated by dividing the stripe spacing of 5.75 mm by the average time interval detected by the laser light system. The ignition energy discharged is 25.4 mJ, which is sufficiently greater than the minimum ignition energy of 0.4 mJ for the stoichiometric propane-air mixture (Lewis and von Elbe, 1987).

Time history of CH-emission intensity from a propagating flame after the spark ignition is measured using a detection unit consisting of a photomultiplier tube (Hamamatsu Photonics R928, a range of sensitive wave length of 185 ~ 900 nm and a maximum sensitivity at 400 nm) and two kinds of optical filters; one is an interference filter with a central wave length of 426.8 nm, a half-width of 14 nm and a maximum transmissivity of 33.7 %, and the other is a usual blue glass filter. The latter is employed to eliminate the influences of background light noise on the quantitative estimation concerning whether CH-light emission is detected.

Optical observations of the wake structure and the behavior of combustion waves are carried out with two types of optical methods; the tomography and the Particle Track Velocimetry (PTV). In the tomography analysis a xenon flash beam with a pulse width of 22 μs passes through a narrow slit and a lens system, and is focused into a light sheet of 1 mm thickness and 25 mm height on the central section perpendicular to the rod axis. In the PTV measurement two consecutive sets of xenon flash lamps with different pulse widths of 38 μs and 13 μs and an interval of 50 μs are combined with the same lens system that used in the tomography analysis. This device enables easy and reliable determination of the direction and speed of particles. In all PTV measurements the first xenon flash can be triggered at an arbitrary delay time after the spark ignition by the same signal that used to trigger the spark discharge.

Smoke of an incense stick is used as tracer particles in the tomography and PTV observations. In Table 1 the specifications of the smoke particles are shown, together with the amplitude response characteristics to the virtual flow oscillation at a frequency of 7.4 kHz, which corresponds to the frequency of Karman vortex shedding behind a rod of 0.3 mm diameter in a uniform velocity stream of U_g = 10 m/s and will be evaluated later in this paper. It is found that the smoke particles have a diameter ranging d_p = 0.1 ~ 1.0 μm and an average density of $\rho_p = 2.2 \times 10^3$ kg/m^3, and can follow to the imposed flow oscillation at a remarkably high value of probability higher than 90 %.

Table 1 Specifications of incense smoke particles

Diameter d_p [μm]	Average density ρ_p [kg/m^3]	Responsibility [%]
0.1 ~ 1.0	2.2×10^3	93.2

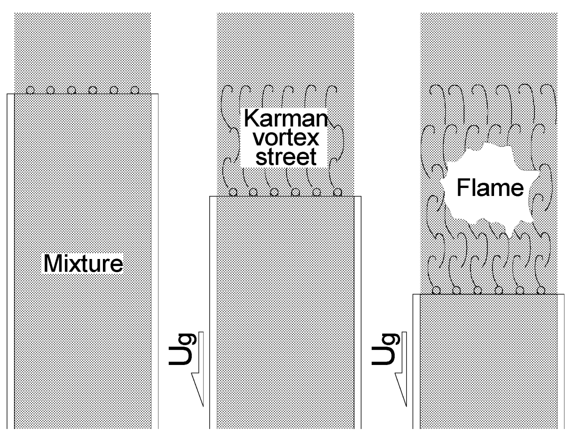

(a) Filling-up of mixture (b) Downward movement of the rod-array (c) Flame propagation after the spark ignition

Fig. 3 Schematic illustrations of the formation process of a quasi-turbulent and quiescent wake and a propagating turbulent premixed flame after the spark ignition

RESULTS AND DISCUSSIONS

Approximate Evaluation of Half-Life Time of Quasi-Turbulent Vortices

To obtain clear figures of the vortex-flame interaction, it is necessary to initiate and propagate a combustion wave in the wake region where sound vortices with moderate tangential velocity prevail. Approximate evaluation of the half-life time of a Karman vortex tube is then attempted so that the time duration suitable for clear observation of the vortex-flame interaction can be quantitatively determined.

Since such small vortices as those generated in this study are greatly affected by the viscosity, Oseen's treatment for a single vortex tube (Aihara, 1984) can be adopted. By denoting the initial vortex diameter by d_0 and the kinetic viscosity by ν, the half-life time of the vortex tangential velocity is given by $t_{1/2} = 3d_0^2/16\nu$. Assuming the initial vortex diameter to be equal to the rod diameter of d_0 = 0.3 mm, using the kinetic viscosity of air at STP of $\nu = 1.56 \times 10^{-5}$ m^2/s, and substituting these values to the above expression, the half-life time is calculated to be $t_{1/2}$ = 1.08 ms. It is found that observations of the vortex-flame interaction should be made within an extremely short time duration of about 1 ms. According to this simplified analysis, optical observations in this study are limited to the initial short time duration of about $t \leq 600$ μs after the spark ignition.

Properties of Quasi-Turbulent and Quiescent Wake

In Fig. 4(a) and (b), a set of a PTV-image and an instanttaneous vector diagram in the cold quasi-turbulent and quiescent wake without combustion is shown, respectively, where the average rod-array velocity is U_g = 10.6 m/s. Particle tracks in Fig. 4(a) indicate that alternately arranged and relatively regular Karman vortex streets prevail in the wake region behind the vertically downward moved rod-array. In the region 4 ~ 10 mm downstream of the rod-array, where premixed flames will be established, many small scale vortices originated from Karman vortex streets are found to exist all over the wake zone. According to picture processing of the vector diagram presented in Fig. 4(b), quantitative details of the quasi-turbulence properties can be estimated and are summarized in the left three columns in Table 2. The characteristic diameter, the tangential velocity and the fundamental frequency of the tangential velocity are shown to take values of l_d = 0.3 mm, v_θ = 4.0 m/s and f_θ (= $v_\theta/\pi l_d$) = 4.2 kHz, respectively.

By assuming that the Strouhal number takes a value of St =

Table 2 Properties of the quasi-turbulent and quiescent vortex tubes

Vortex diameter l_d [mm]	Tangential velocity v_θ [m/s]	Tangential frequency f_θ [kHz]	Scale ratio l_d/δ_L	Velocity ratio v_θ/S_L
0.3	4.0	4.2	1.3 ~ 3.3 (1.0)	5.3 ~ 11 (10)

0.21 (Schlichting, 1979) for the wake behind a single rod of 0.3 mm diameter in the uniform stream of a velocity of U_g = 10.6 m/s, the shedding frequency of Karman vortex street is calculated to be f_0 = 7.4 kHz. Also assuming that the tangential velocity of Karman vortex approximately corresponds to the maximum turbulence intensity in the wake, which takes a value of 20 ~ 40 % of the uniform velocity (Kumada et al., 1984), it can be evaluated to be v_θ = 2.1 ~ 4.2 m/s. These values exhibit reasonable agreement with those obtained above.

According to these quantitative results, it can be noted here that the proposed apparatus described above has the following valuable and interesting advantages. The rod diameter exerts direct influences on the turbulence scale of Karman vortex streets, whereas the average rod-array velocity has great influences on their turbulence intensity. The pitch of rod-array, on the other hand, adjusts the degree of interrelation among neighboring Karman vortex streets. Therefore, by varying the quantitative combination of three parameters; the rod diameter d_0, the average rod velocity U_g and the pitch of rod-array s, the proposed equipment can realize an extremely wide range of turbulence characteristics. It is found that the quantitative combination of d_0 = 0.3 mm, U_g = 10 m/s and s = 0.6 mm adopted in this paper as the first step of investigation produces relatively small and intense turbulence characteristics, the former being comparable with the flame thickness.

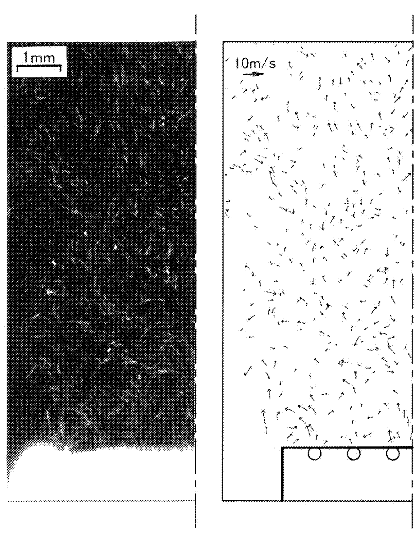

(a) PTV-image (b) Vector diagram

Fig. 4 An example of (a) PTV-image and (b) vector diagram of the cold quasi-turbulent and quiescent wake, where the rod-array velocity is U_g = 10.6 m/s

Time Variations of CH-Emission Intensity from Propagating Flames

In order to discuss the appearances and behavior of the combustion waves based on the optical observations, it is indispensable to certify first whether the interfaces focused on the tomograph images really correspond to the flame surfaces. Since the detection of CH-light emission in the hydrocarbon-fuelled combustion is equivalent to the existence of the reacting flame (Haker, 1967), the intensity fluctuation of CH-emission from the propagating flames after the spark ignition is measured. The results are given in Fig. 5, where the solid line indicates the CH-emission intensity profile of the spark-ignited turbulent flame in the quasi-turbulent and quiescent wake with U_g = 10.5 m/s, the broken line gives that of the spark-ignited laminar flame propagating in the quiescent mixture, and the dotted line presents that of the electric spark in the open atmosphere without combustion.

Since no signal such as electric noise is detected when the perfect optical shield is made on the photo-multiplier, it is found that the electric spark in the atmosphere generates definite but quickly dumping light around a wave length of CH-emission in a short period of $t \leq 140$ µs. Compared with the spark light emission given by the dotted line, the profiles of CH-emission from the laminar and turbulent flames exhibit

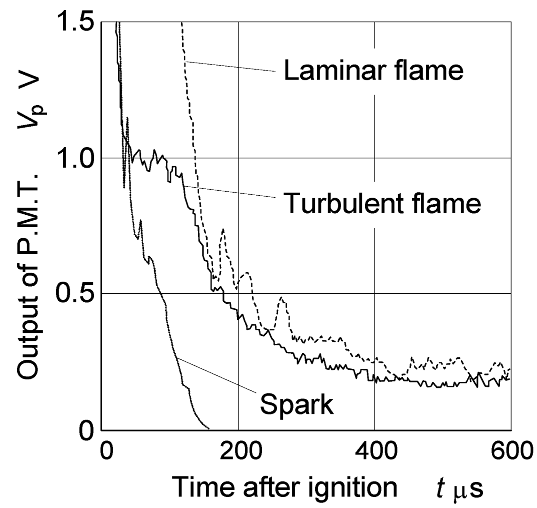

Fig. 5 Time histories of CH-emission intensity from three kinds of light sources; laminar flame, turbulent flame and electric spark

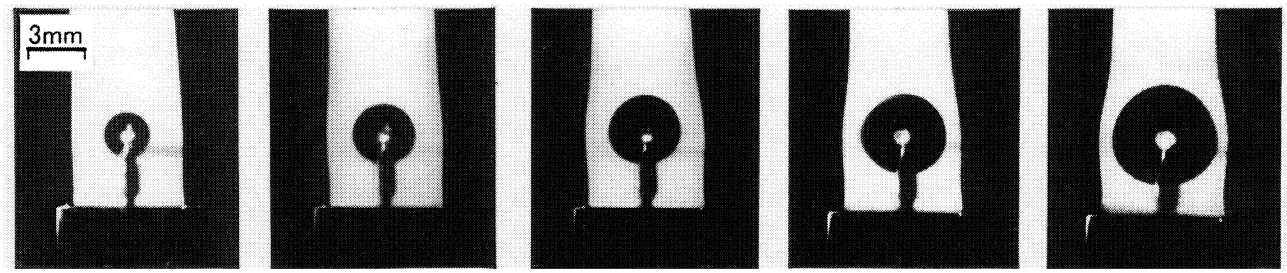

$t = 98$ μs $t = 208$ μs $t = 308$ μs $t = 396$ μs $t = 506$ μs

(a) A set of tomograph images of a laminar flame propagating in the quiescent mixture

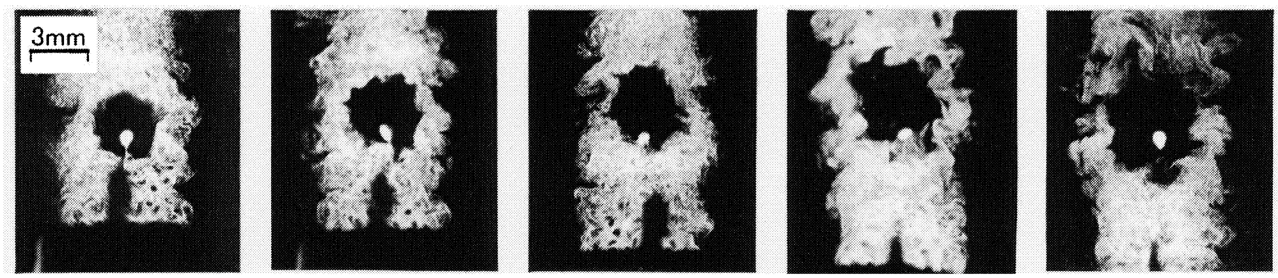

$t = 100$ μs $t = 208$ μs $t = 300$ μs $t = 406$ μs $t = 496$ μs

(b) A set of tomograph images of a turbulent flame propagating in the quasi-turbulent and quiescent wake

Fig. 6 Five sets of tomograph images of (a) propagating laminar flames in the quiescent mixture and (b) propagating flames in the quasi-turbulent and quiescent wake, where the average rod-array velocity is $U_g = 10.5$ m/s

enough intensity to certify the existence of the flame during the observation period less than 600 μs after the spark ignition. In the following paragraphs, therefore, examinations and discussions concerning the experimental results are made by considering the interfaces observed in the tomograph images as the propagating flame surfaces.

According to further comparison of the profile of CH-emission intensity of the laminar flame with that of the turbulent one, it is found that the former emits more intense CH-light in the earlier stage of the flame propagation than the latter. This suggests the existence of strong cooling effect by the quasi-turbulent vortices on the incipient formation stage of a combustion wave.

Tomography Observations of Spark-Ignited Laminar and Turbulent Flames

A set of five instantaneous tomograph images of a laminar combustion wave formed in the quiescent mixture and that of a turbulent combustion wave in the quasi-turbulent and quiescent wake are shown in Fig. 6(a) and (b), respectively. The average rod-array velocity in Fig. 6(b) is set at $U_g = 10.5$ m/s. As already shown concerning Fig. 2, all images are separately taken from the direction parallel to the rod axis at about 100 μs time intervals. In Fig. 6, the white zone indicates the unburnt mixture region, the left- and right-side black zones give the atmospheric region, and the central black zone with a smooth or a rugged interface at its surroundings gives the burnt gas region.

A spherically expanding combustion wave with a smooth interface can be observed in each image in Fig. 6(a), being particular to the laminar premixed flame. The propagating velocity of the combustion wave, which is called the flame speed and denoted by S_F, is estimated to be $S_F = 2.1 \sim 4.5$ m/s. Assuming here the density ratio to be $\rho_u/\rho_b = 6.0$, where ρ_u and ρ_b indicate densities of the unburnt mixture and burnt gas, respectively, results in the laminar burning velocity ranging $S_L = 35 \sim 75$ cm/s for the stoichiometric propane-air mixture, indicating reasonable agreement with the experimental results (Harries et al., 1949, Chigier, 1981, Glassman, 1987, Hill and Hung, 1988).

Images of the turbulent flame formed in the quasi-turbulent and quiescent wake given in Fig. 6(b), on the other hand, show that a smooth circular laminar combustion wave is completely crumpled up by the quasi-turbulent vortices into a complex and wrinkled interface between the unburnt and burnt gases. It is also found that the rugged interface between the white zone and the central black zone is composed of a series of wrinkles having a length scale of $0.2 \sim 2$ mm, being of same order as that of the quasi-turbulent vortices. Therefore, further analysis of the concrete relationship between the flame properties and the quasi-turbulence characteristics is expected to provide some key factors for elucidating the enhancement mechanism of the flame propagation by the vortex-flame interaction. Taking the experimental certification by CH-emission measurements into consideration, the wrinkled interface is found to correspond to the propagating flame surface and is classified into the finely wrinkled laminar flame.

Relation between Turbulence Characteristics and Flame Structure

Detailed and careful observation of Fig. 6(b) exhibits an important characteristic feature concerning the quasi-turbulent and quiescent wake employed in this investigation. Karman vortex streets can be clearly distinguished in the lower part of the white zone as an alternative array of small black points, and their diameters are measured to have almost same value ranging $l_d = 0.2 \sim 0.5$ mm as that of the rod diameter of 0.3 mm. According to Williams (1984) and Glassman (1987), the laminar flame thickness is roughly estimated as $\delta_L = a/S_L = 0.1 \sim 0.2 \approx 0.15$ mm, by using the thermal diffusivity of air of $a = 3.0 \times 10^{-4}$ m^2/s at 1200 °C and 1 atm and the measured laminar burning velocity of $S_L = 35 \sim 75$ cm/s. Since the vortex tangential velocity is already estimated to be $v_\theta = 4.0$ m/s, these quantitative results give a rather small turbulence length scale of $l_d/\delta_L = 1.3 \sim 3.3$, having an order of 1.0, and a relatively intense turbulence velocity of $v_\theta/S_L = 5.3 \sim 11$, having an order of 10. These numerical ranges and orders are listed in the right two columns of Table 2.

It is summarized that, by employing the rod diameter of 0.3 mm, the average rod velocity of about 10 m/s and the rod pitch of 0.6 mm, the proposed experimental apparatus can realize such valuable turbulence fields that consist of a regular array of small and moderately intense vortex tubes. They have a rather small characteristic length scale nearly equal to the laminar flame thickness and relatively intense vortex strength about an order of magnitude greater than the laminar burning velocity; $l_d/\delta_L \approx 1$ and $v_\theta/S_{L,m} \approx 10$. It is concluded therefore that, by interacting with an array of vortex tubes having rather small and intense turbulence conditions of $l_d/\delta_L \approx 1$ and $v_\theta/S_{L,m} \approx 10$, a smooth laminar combustion wave is crumpled up into a finely wrinkled laminar flame consisting of a continuous series of complex and rugged flame elements.

CONCLUDING REMARKS

In this paper the spark-ignited turbulent premixed flames are generated in the quasi-turbulent and quiescent wake, which is formed by rapidly moving the rod-array vertically downward in the stoichiometric propane-air mixture. The tomography and PTV are employed to observe the structure and behavior of propagating flames. Measurement of CH-emission intensity is also made. Observations and analyses are restricted to the initial short time duration of 600 μs after the spark ignition, based on the approximate quantitative evaluation of the half-life time of the quasi-turbulent vortex. The results in this paper are summarized as follows.

(1) The proposed quasi-turbulent and quiescent wake is found to be composed of an alternative array of Karman vortex streets having an almost same length scale ranging $l_d = 0.2 \sim 0.5$ mm as that of the rod diameter of 0.3 mm. This results in a rather small turbulence scale of $l_d/\delta_L \approx 1$.

(2) Based on the PTV measurements, the tangential velocity of the quasi-turbulent vortex tubes is estimated to be $v_\theta = 4.0$ m/s. The mean laminar burning velocity is also evaluated to be 55 cm/s by processing the tomograph images. This yields a rather intense turbulence condition of $v_\theta/S_L \approx 10$. The realized quasi-turbulent and quiescent wake is found to produce the moderately intense turbulence condition of $v_\theta/S_L \approx 10$.

(3) Interacting with an alternative array of Karman vortex streets as it propagates in the quasi-turbulent and quiescent wake, a spherical laminar combustion wave is crumpled up into a complex and rugged interface consisting of fine wrinkles of a length scale ranging 0.2 ~ 2 mm. It is concluded therefore that the turbulent flame established in the proposed quasi- turbulent and quiescent wake with the relatively small and moderately intense turbulence conditions of $l_d/\delta_L \approx 1$ and $v_\theta/S_L \approx 10$ is classified into the finely wrinkled laminar flame.

REFERENCES

Aihara, Y., *Mechanics of Fluid Flow* (in Japanese), 1st ed., (1984), p. 53, Baifukan.

Ballal, D. R. and Lefevre, A. H., *Proceedings of Royal Society of London*, Ser. A, 344, (1975), pp. 217-234.

Bradley, D., *Proceedings of Combustion Institute*, **24**, (1992), pp. 247-262.

Chigier, N., *Energy, Combustion, and Environment*, (1981), p. 118, McGraw Hill.

Glassman, I., *Combustion*, 2nd ed., (1987), p.137 and p. 117, Academic Press.

Haker, J. H., *Journal of Institute of Fuel*, **40**-316, (1967), p.206.

Harries, M. E., Grumer, J., von Elbe, G. and Lewis, B., *Third International Symposium on Combustion, Flame and Explosion Phenomena*, (1949), pp. 80-89, Williams & Wilkins, Baltimore.

Hill, P. G. and Hung, J., *Combustion Science and Technology*, **60**-1, (1988), p.7.

Kumada, M., Hiwada, M., Ito, M., and Mabuchi, I., *Transactions of JSME* (in Japanese), **50**-455B, (1984), pp. 1699-1706.

Lewis, B. and von Elbe, G., *Combustion, Flames and Explosions of Gases*, 3rd ed.,, (1987), p. 345, Academic Press.

Peters, N., *Journal of Fluid Mechanics*, **384**, (1999), pp. 107-132.

Poinsot, T., Veynante, D. and Candel, S., *Journal of Fluid Mechanics*, **288**, (1991), pp. 561-606.

Schlichting, H., (Translated by Kestin, J.), *Boundary-Layer Theory*, 7th ed., (1979), p. 31, McGraw Hill.

Williams, F. A., *Combustion Theory*, 2nd ed., (1984), p. 135, Benjamin/Cummings.